Changes in the Midpoint Potentials of the Nitrogenase Metal Centers as a Result of Iron Protein−Molybdenum-Iron Protein Complex Formation†

William N. Lanzilotta and Lance C. Seefeldt*

Department of Chemistry and Biochemistry, Utah State University, Logan, Utah 84322

Received June 25, 1997; Revised Manuscript Received August 5, 1997⊗

ABSTRACT: All nitrogenase-catalyzed substrate reduction reactions require the transient association between the iron (Fe) protein component and the molybdenum-iron (MoFe) protein component with concomitant intercomponent electron transfer and MgATP hydrolysis. Understanding the effects of Fe protein−MoFe protein complex formation on the properties of the nitrogenase metal centers is thus essential to understanding the electron transfer reactions. This work presents evidence for significant shifts in midpoint potentials for two of the three nitrogenase metal centers as a result of Fe protein binding to the MoFe protein. The midpoint potentials for the three nitrogenase metal centers, namely the [4Fe-4S] cluster of the Fe protein, and the [8Fe-7S] (or P−) clusters and FeMo cofactors (or M-centers) of the MoFe protein, were determined within a nondissociating nitrogenase complex prepared with a site-specifically altered Fe protein (Leu at position 127 deleted, L127Δ). The midpoint potential for each metal center was determined by mediated redox titrations, with the redox state of each center being monitored by parallel and perpendicular mode EPR spectroscopy. The midpoint potential of the Fe protein $[4Fe\text{-}4S]^{2+/1+}$ cluster couple was observed to change by −200 mV from −420 mV in the uncomplexed L127Δ Fe protein to −620 mV in the L127Δ Fe protein−MoFe protein complex. The midpoint potential of the two electron oxidized couple of the P-clusters ($P^{2+/N}$) of the MoFe protein was observed to shift by −80 mV upon protein−protein complex formation. No significant change in the midpoint potential of an oxidized state of FeMoco ($M^{ox/N}$) was observed upon complex formation. These results provide insights into the energetics of intercomponent electron transfer in nitrogenase, suggesting that the energy of protein−protein complex formation is coupled to an increase in the driving force for electron transfer. The results are interpreted in light of the expected changes in the protein environments of the metal centers within the nitrogenase complex.

Nitrogenase catalyzed substrate reduction reactions require the transient association of the two nitrogenase component proteins, the iron (Fe) protein[1] and the molybdenum-iron (MoFe) protein, with the transfer of one electron between the proteins being coupled to the hydrolysis of MgATP (*1*−*5*). Following electron transfer, the two component proteins dissociate in what appears to be the overall reaction rate limiting step (*6*−*8*). The dissociated, oxidized Fe protein is reduced by flavodoxin or ferredoxin, and the two MgADP molecules are replaced by two MgATP molecules. This cycle is repeated until sufficient electrons have accumulated in the MoFe protein for substrate reduction (*5*). The flow of electrons through nitrogenase appears to be from the [4Fe-4S] cluster of the Fe protein to an [8Fe-7S] (or P-) cluster of the MoFe protein, and finally to a molybdenum-iron-sulfur-homocitrate cofactor (FeMoco or M-cluster) of the MoFe protein, the site of substrate binding and reduction (*9*, *10*).

Defining the properties of the nitrogenase metal centers is essential to understanding the nitrogenase mechanism. While much is known about each of the metal centers in the uncomplexed component proteins (*7*), little is known about the properties of the centers within the Fe protein−MoFe protein complex, a state that is relevant for all nitrogenase reactions. Given the location of two of the nitrogenase metal centers (the [4Fe-4S] cluster and the P-cluster) near the component protein docking interface (*11*), it is expected that protein−protein complex formation will alter the properties of these metal centers. Of particular interest would be how complex formation affects the midpoint potentials of the metal centers and hence the driving force for electron transfer between the centers.

In the free Fe protein, the [4Fe-4S] cluster is bridged between the two identical subunits near one end of the Fe protein, with significant solvent exposure (*12*). The relevant oxidation states of the [4Fe-4S] cluster are the 2+/1+ couple,[2] with a measured midpoint potential (E_m) of approximately −300 mV (*13*). It has recently been observed that the [4Fe-4S] cluster of the Fe protein can be reduced to an all ferrous (0) state, although the role of the 1+/0 couple

† This work was supported by National Science Foundation Grant MCB-9722937. The Bruker ESP300E EPR spectrometer was purchased with funds provided by the National Science Foundation (BIR-9413530) and Utah State University.

* Address correspondence to this author. Phone: (801) 797-3964. Fax: (801) 797−3390. Email: seefeldt@cc.usu.edu.

⊗ Abstract published in *Advance ACS Abstracts,* October 1, 1997.

[1] Abbreviations: Fe protein, iron protein of nitrogenase; MoFe protein, molybdenum-iron protein of nitrogenase; L127Δ Fe protein, Fe protein with Leu 127 deleted; EPR, electron paramagnetic resonance; P-cluster, [8Fe-7S] cluster of nitrogenase; M-cluster, FeMo cofactor of nitrogenase; IDS, indigo disulfonate; MOPS, 3-(*N*-morpholino)-propanesulfonic acid; E_m, midpoint potential; tricine, *N*-[tris-(hydroxymethyl)methyl]glycine.

[2] The redox couples of low-potential [4Fe-4S] clusters can also be defined in terms of the formal charges of the entire cluster $[4Fe\text{-}4S\text{-}(Cys)_4]$ where the $2^+/1^+$ couple corresponds to net charges of $2^-/3^-$.

S0006-2960(97)01537-7 CCC: $14.00

in electron transfer is not clear (*14*). Significantly, MgATP or MgADP binding to the Fe protein has been shown to influence the spectroscopic and electronic properties of the [4Fe-4S] cluster (*15*−*19*), resulting in the lowering of the E_m to −420 mV upon MgATP binding or to −460 mV upon MgADP binding (*13*, *20*). The exact role of nucleotide-dependent lowering of the midpoint potential in electron transfer is not known.

The P-clusters of the MoFe protein are [8Fe-7S] clusters bound between the α and β subunits, near the protein surface (*21*). Several lines of evidence suggest that the P-clusters are the immediate electron acceptors from the [4Fe-4S] cluster of the Fe protein, which include their location at the Fe protein docking site (*11*) and recent spectroscopic studies (*22*−*25*). The relevant oxidation states of the P-clusters in electron transfer are not, however, clear. When the MoFe protein is isolated in the presence of the reductant dithionite, the P-cluster oxidation state (designated as P^N) has all of the iron atoms in the ferrous state (*26*−*28*). Since further reduction is unlikely, current thought is that more oxidized states are probably relevant to electron transfer (*24*). This idea is supported by recent X-ray crystal structural analysis of different oxidation states of the P-cluster, which revealed ligation state changes upon oxidation and reduction (*29*). In addition, spectroscopic evidence has revealed that the P-clusters become oxidized during N_2 reduction (*24*). The P-clusters can be oxidized by up to six electrons from the P^N state, with the first three oxidations being reversible (*30*, *31*). These states have been designated as P^{1+}, P^{2+} and P^{3+}, with measured E_m values for the three couples of −307, −307, and +90 mV, respectively (*30*, *32*).

FeMoco of nitrogenase is a [7Fe-9S-1Mo-1homocitrate] center that can be oxidized or reduced from the resting state (M^N) by multiple electrons, with the first oxidized couple M^{ox}/M^N having a measured midpoint potential of −42 mV (*30*). More reduced states of FeMoco (M^R) appear to require specific reduction by the Fe protein, and little is known about the midpoint potentials for these couples.

In the present work, we have established the midpoint potentials (E_m) for the nitrogenase metal centers within a nondissociating, electron transfer competent Fe protein−MoFe protein complex created by alteration of an amino acid within the Fe protein (deletion of a Leu at position 127). Significant changes in the E_m for the Fe protein [4Fe-4S] cluster and MoFe protein P-cluster were observed to result from protein−protein docking, suggesting that complex formation plays an important role in defining the driving force for electron transfer between the nitrogenase component proteins.

EXPERIMENTAL PROCEDURES

Site-Directed Mutagenesis, Expression, and Purification of Nitrogenase and Flavodoxin. Wild-type nitrogenase Fe and MoFe proteins were purified from *Azotobacter vinelandii* cells essentially as described (*33*). Site-directed mutagenesis of the gene that encodes the subunits of the Fe protein of *A. vinelandii*, *nif H*, was performed as described (*33*). The L127Δ Fe protein was expressed and purified as before (*33*, *34*). Flavodoxin II was purified from *A. vinelandii* cells essentially as described (*35*). All purified proteins were homogeneous as determined by coomassie blue staining of SDS gels (*36*). Protein concentrations were determined by a modified biuret method (*37*), with bovine serum albumin as the standard. Nitrogenase acetylene reduction rates were determined as described (*33*, *38*), and both the Fe protein and the MoFe protein had specific activities greater than 2000 nmol of acetylene reduced min^{-1} (mg of protein)$^{-1}$. No acetylene reduction activity was detected for the L127Δ Fe protein when combined with the MoFe protein. Flavodoxin II concentrations were also determined from the known absorption coefficient for the quinone oxidation state of 11.3 mM^{-1} cm^{-1} at 452 nm (*35*). All sample manipulations were carried out in an argon filled glove box (Vacuum Atmospheres, Hawthorne, CA) with less than 1 ppm oxygen. All buffers were purged with argon.

Sample Preparation for EPR Spectroscopy. Electron transfer from the L127Δ Fe protein to the MoFe protein was monitored by EPR spectroscopy essentially as previously described (*39*). L127Δ Fe protein and MoFe protein were passed through a Sephadex G-25 column equilibrated with 100 mM MOPS buffer, pH 7.0, containing 150 mM NaCl and 2 mM sodium dithionite. Flavodoxin II was reduced with titanium (III) citrate (*38*) to the hydroquinone oxidation state, followed by separation from the titanium citrate by passage through a P-4 column (Bio-Rad, Richmond, CA) equilibrated with 100 mM MOPS buffer, pH 7.0. Three separate protein solutions were prepared in 100 mM MOPS buffer, pH 7.0: (1) MoFe protein alone (67 μM), (2) Fe protein alone (150 μM), and (3) MoFe protein (67 μM) and Fe protein (150 μM). Each solution was allowed to incubate for 15 min at 25 °C prior to freezing an aliquot into an EPR tube. To the remaining aliquot of sample 3 above, reduced flavodoxin II (hydroquinone) was added to a final concentration of 200 μM, and the sample was allowed to react for 15 min at 25 °C, and then it was frozen in an EPR tube.

Redox Titrations. Potentiometric titrations were performed essentially as previously described (*40*) in 50 mM Tricine buffer, pH 8.0, including 50 μM each of a series of redox mediators. For titrations below −500 mV, the mediators included flavin mononucleotide (E_m = −172 and −238 mV), benzyl viologen (E_m = −361 mV), methyl viologen (E_m = −440 mV) and *N*,*N*′-propane-2,2′-dipyridinium (E_m = −590 mV; a gift from Dr. Vernon Parker, Utah State University). For titrations in the potential range from +100 to −300 mV, the mediators included methylene blue (E_m = + 11 mV), indigo disulfonate (IDS) (E_m = −125 mV), flavin mononucleotide, and benzyl viologen. The redox potential of the mediator solution was adjusted by the addition of aliquots of a 5 mM dithionite ($Na_2S_2O_4$) solution, a 5 mM indigo disulfonate solution, or a 5 mM potassium ferricyanide solution. For titrations below −500 mV, reduction was accomplished in a standard H-cell using a Hewlett-Packard 6212C constant power supply with a gold wire working electrode and a platinum mesh counter electrode (2 cm × 1 cm). In all cases, the reference electrode was a Ag/AgCl microelectrode that was calibrated against a standard calomel electrode. Aliquots at defined potentials were removed and frozen in calibrated EPR tubes. All potentials are reported relative to the normal hydrogen electrode (NHE). The relative concentration of the reduced and oxidized states for each metal center were determined by the peak-to-peak height of the appropriate EPR signal. A plot of the relative fraction of the metal cluster reduced versus the applied potential was fit to the Nernst equation (*20*) using the nonlinear, least squares fitting program Igor Pro (Wavemet-

ics, Lake Oswego, OR).

EPR Spectroscopy. EPR spectra were recorded on a Bruker ESP300E spectrometer equipped with a dual mode cavity and an Oxford ESR 900 liquid helium cryostat. In all cases, 4 mm calibrated quartz EPR tubes (Wilmad, Buena, NJ) were used. EPR spectra acquired in perpendicular mode were recorded with a microwave frequency of 9.64 GHz, a microwave power of 10.1 mW, a modulation frequency of 100.0 kHz, a modulation amplitude of 5.028 G, a conversion time of 5.12 ms, a time constant of 10.24 ms, and a temperature of 12 K. In each case, the final spectrum was the sum of 10 scans. Spectra acquired in parallel mode were recorded with a microwave frequency of 9.35 GHz, a microwave power of 20 mW, a modulation frequency of 100 kHz, a modulation amplitude of 7.969 G, a conversion time of 5.12 ms, a time constant of 10.24 ms, and a temperature of 12 K. In each case, the final spectrum was the sum of 20 scans.

RESULTS

Reduction of the Fe Protein [4Fe-4S] Cluster within a Nitrogenase Complex. Several lines of evidence suggest that the properties of the Fe protein [4Fe-4S] cluster change upon Fe protein binding to the MoFe protein. For example, during the transient association of the Fe protein with the MoFe protein following intercomponent electron transfer, a significant fraction of the Fe protein [4Fe-4S] cluster is observed to be in the oxidized (2+) state by visible and EPR spectroscopies even when the reaction is carried out in the presence of the reductant dithionite (*6*). This is somewhat surprising since dithionite will rapidly reduce the oxidized $[4Fe\text{-}4S]^{2+}$ cluster of the Fe protein when this protein is not complexed with the MoFe protein (*6*). Thus, the appearance of the oxidized $[4Fe\text{-}4S]^{2+}$ cluster while the Fe protein is bound to the MoFe protein suggests that dithionite is unable to reduce the [4Fe-4S] cluster while the two component proteins are docked. This has been interpreted as MoFe protein blocking access of dithionite to the [4Fe-4S] cluster of the Fe protein (*6*, *41*).

A similar observation is illustrated from studies on the metal centers of nitrogenase within a nondissociating Fe protein−MoFe protein complex (*39*). It has been observed that deletion of an amino acid within a MgATP signal transduction switch motif of the Fe protein (Leu 127Δ) induced protein conformational changes similar to those normally induced by MgATP-binding (*34*). This L127Δ Fe protein has an extremely high affinity for binding to the MoFe protein even in the absence of nucleotides, forming an essentially nondissociating Fe protein−MoFe protein complex (*39*). Interestingly, a single electron is transferred from the L127Δ Fe protein [4Fe-4S] cluster to the P-cluster of the MoFe protein in a reaction that does not require MgATP (*39*). Following this electron transfer reaction, the oxidized $[4Fe\text{-}4S]^{2+}$ cluster of the L127Δ Fe protein remains in the oxidized state even when the complex is incubated in an excess of the reductant dithionite (*39*). The presence of the oxidized or reduced state of the [4Fe-4S] cluster can be monitored by the increased absorption at 430 nm in the visible spectrum for the oxidized cluster, or by the disappearance of the $g = 1.94$ centered EPR spectrum of the $S = 1/2$ reduced [4Fe-4S] cluster in going to the $S = 0$ oxidized (2+) state. Figure 1 (trace 1) illustrates the low-temperature

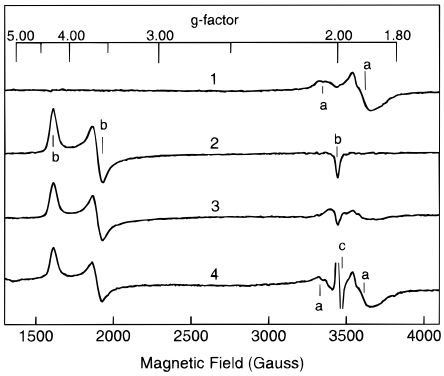

FIGURE 1: Reduction of the Fe protein [4Fe-4S] cluster within a nitrogenase complex. Perpendicular mode EPR spectra were recorded as described under Experimental Procedures. Four samples were prepared: trace 1, L127Δ Fe protein (150 μM) alone; trace 2, MoFe protein (67 μM) alone; trace 3, L127Δ Fe protein (150 μM) with MoFe protein (67 μM); and trace 4, an aliquot of the sample used for trace 3 to which reduced flavodoxin II had been added to a final concentration of 200 μM. All samples were allowed to incubate for 15 min at 25 °C prior to freezing in EPR tubes. The sample in trace 4 was allowed to incubate an additional 15 min at 25 °C following the addition of flavodoxin II. The signals arising from the L127Δ Fe protein $[4Fe\text{-}4S]^{1+}$ cluster are marked as a, the signals from reduced FeMoco are marked as b, and the flavodoxin semiquinone radical signal is marked as c.

EPR spectrum observed for the L127Δ Fe protein when the protein was incubated in the presence of the reductant dithionite. The inflections centered around $g = 1.94$ (denoted by "a") result from the reduced (1+) state of the [4Fe-4S] cluster. When the L127Δ Fe protein is mixed with the MoFe protein, the transfer of an electron from the [4Fe-4S] cluster to the MoFe protein leaves the [4Fe-4S] cluster in the oxidized (2+), EPR silent state. This can be seen in Figure 1 (trace 3) by the disappearance of the EPR signals resulting from the reduced [4Fe-4S] cluster (disappearance of the inflections marked a). The EPR signals arising from the reduced FeMoco (marked b) remain essentially unchanged between the uncomplexed (trace 2) and complexed (trace 3) states. Importantly, the [4Fe-4S] cluster is in the oxidized state when the L127Δ Fe protein is bound to the MoFe protein even in the presence of the reductant dithionite. These results indicate that when the Fe protein is bound to the MoFe protein, dithionite is not able to reduce the oxidized [4Fe-4S] cluster.

It seemed possible that electron transfer mediators other than dithionite might be able to reduce the oxidized [4Fe-4S] cluster within the nitrogenase complex. *A. vinelandii* flavodoxin II is a small FMN containing protein (*35*) that is known to rapidly reduce the [4Fe-4S] cluster of the Fe protein (*42*). The hydroquinone/semiquinone couple of flavodoxin II has a midpoint potential of −515 mV at pH 8.0 (*35*, *43*). Figure 1 (trace 4) illustrates the effect of adding reduced flavodoxin II to the L127Δ Fe protein−MoFe protein complex following electron transfer. As can be seen, the EPR inflections centered at $g = 1.94$ (marked a) resulting from the reduced state of the [4Fe-4S] cluster reappear upon addition of flavodoxin as a reductant. These results suggest that flavodoxin can reduce the [4Fe-4S] cluster within the L127Δ−MoFe protein complex, whereas dithionite cannot. In separate experiments, it has been confirmed that flavodoxin does not simply stimulate the dissociation of the L127Δ Fe protein from the MoFe protein (*39*).

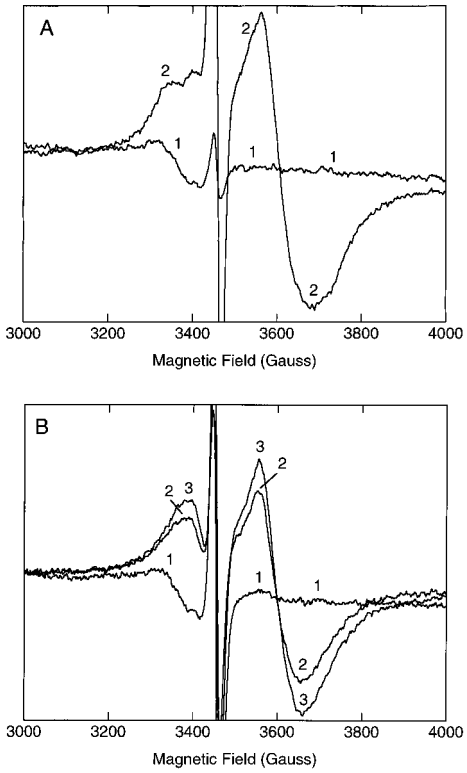

FIGURE 2: EPR spectra of L127Δ Fe protein and L127Δ Fe protein complexed with MoFe protein at different potentials. Samples of L127Δ Fe protein alone (panel A) and L127Δ Fe protein complexed to the MoFe protein (panel B) were poised at different redox potentials before being frozen in EPR tubes as described under Experimental Procedures. (Panel A) EPR spectra of L127Δ Fe protein at −290 mV (trace 1) and −534 mV (trace 2). No further changes in the EPR signal intensity were observed below −534 mV. (Panel B) EPR spectra of the L127Δ Fe protein−MoFe protein complex at −530 mV (trace 1) and −730 mV (trace 2). A sample was also prepared at −700 mV in the presence of flavodoxin II (trace 3). No further changes in the EPR signal intensity were observed below −700 mV. All EPR spectra were recorded in perpendicular mode as described. The radical signals at center field arise from the cation radical state of the viologens and the semiquinone oxidation state of flavodoxin II. Spin integration of the signals in panel B indicate that 88% (trace 3) and 73% (trace 2) of the $[4Fe\text{-}4S]^{1+}$ EPR signal is present compared to trace 2 in panel A.

It was possible that the reduction of the $[4Fe\text{-}4S]^{2+}$ cluster within the L127Δ Fe protein−MoFe protein complex could only be catalyzed by flavodoxin II. To test this possibility, the L127Δ Fe protein−MoFe protein complex, with the [4Fe-4S] cluster in the oxidized state, was incubated with a combination of redox mediators at defined potentials, either in the presence or in the absence of flavodoxin II. The oxidation state of the [4Fe-4S] cluster was monitored from the intensity of the $g = 1.94$ centered EPR signal of the 1+ oxidation state. Figure 2 illustrates that the oxidized state of the [4Fe-4S] cluster of the Fe protein was reduced at negative potentials either with or without flavodoxin II. Notably, a much more negative redox potential was required to reduce the $[4Fe\text{-}4S]^{2+}$ cluster when the Fe protein was bound to the MoFe protein than in the control with the Fe protein alone (compare panels A and B), suggesting that complex formation induces a negative shift in the [4Fe-4S] cluster midpoint potential. It is also clear that flavodoxin II is not absolutely required for reduction of the [4Fe-4S] cluster within the complex, although its presence did appear to result in a slightly greater percentage of the [4Fe-4S] cluster being reduced. This effect could result from stabilization of the L127Δ Fe protein under the electrochemical reduction conditions.

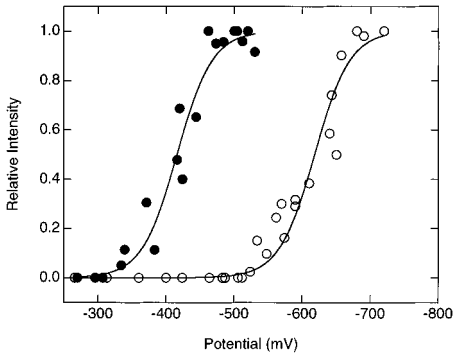

FIGURE 3: Redox titrations of the L127Δ Fe protein [4Fe-4S] cluster. Electrochemical redox titrations were performed as outlined under Experimental Procedures for the $[4Fe\text{-}4S]^{2+/1+}$ couple in the L127Δ Fe protein alone (●) and in the L127Δ Fe protein complexed to the MoFe protein (○). The 1+ oxidation state of the Fe protein [4Fe-4S] cluster was monitored from the intensity of the $S = {}^1/_2$ EPR signal. The signal peak-to-peak height was normalized to the maximum height observed at the lowest potential. The solid lines represent nonlinear least-squares fits of the data to the Nernst equation where n = 1, and the calculated midpoint potentials were found to be −420 and −620 mV, respectively.

The observation that the oxidized [4Fe-4S] cluster of the L127Δ Fe protein could be reduced by mediators within the nitrogenase complex offered the possibility of establishing the midpoint potential of this cluster using mediated redox titrations monitored by EPR spectroscopy (*34*). Figure 3 presents redox titrations for the 2+/1+ couple of the [4Fe-4S] cluster of L127Δ Fe protein either in the uncomplexed state or in the MoFe protein complexed state. From fits of the data to the Nernst equation (*34*), E_m values of −420 and −620 mV were determined for these two states of the Fe protein, respectively. The E_m value measured for the L127Δ Fe protein alone of −420 mV is consistent with earlier published values (*34*). The observed shift in the E_m to −620 mV upon protein−protein complex formation represents a −200 mV change that can be ascribed to protein−protein docking. This is the largest change in midpoint potential observed for a redox center upon protein partner complex formation.

Titration of the MoFe Protein M- and P-Clusters within a Nitrogenase Complex. Given the large change in the E_m value for the Fe protein [4Fe-4S] cluster upon protein−protein docking and the location of the P-clusters of the MoFe protein at the docking interface (*11*), it was important to establish the midpoint potential of the P-clusters within the docked complex. The three oxidation states of the P-cluster designated as P^N, P^{1+}, and P^{2+} are readily accessible and reversible with measured midpoint potentials of −307 mV for both the P^N/P^{1+} and P^{1+}/P^{2+} couples (*30*, *31*, *44*−*46*). It is possible to monitor the reduction of the P^{2+} oxidation state to the P^N oxidation state by the disappearance of a $g = 11.8$ parallel mode EPR signal (*25*). Using mediated redox titrations (*34*) and parallel mode EPR, the midpoint potential of the P-clusters (either when the MoFe protein was alone or when bound to the L127Δ Fe protein) was established. Figure 4 illustrates typical redox titrations for the P^{2+}/P^N cluster couple. The data were fit to the Nernst equation for a two electron process ($n = 2$, solid lines), since earlier studies indicated that the P^{2+}/P^{1+} and P^{1+}/P^N couples

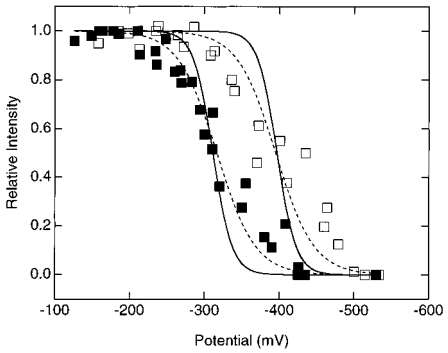

FIGURE 4: Redox titrations of the MoFe protein P-clusters. Electrochemical redox titrations were performed as outlined under Experimental Procedures for the $P^{2+/N}$ couple in the MoFe protein alone (■) and in the MoFe protein complexed to the L127Δ Fe protein (□). The P^{2+} oxidation state of the P-cluster was monitored by the intensity of the $S \geq 3$ parallel mode EPR signal. The signal peak height was normalized to the maximum peak height observed at the most positive potential. The solid lines represent nonlinear least-squares fits of the data to the Nernst equation where $n = 2$, and the calculated midpoint potentials were found to be −310 and −390 mV, respectively. The dashed lines represent nonlinear least-squares fits of the data to the Nernst equation where $n = 1$ and the calculated E_m values are the same as for the fits with $n = 2$.

have nearly identical E_m values, requiring 2 equiv of electrons to reduce the P^{2+} oxidation state. E_m values of −310 mV for the MoFe protein alone and −390 mV for the MoFe protein when bound to the L127Δ Fe protein were determined. Interestingly, the Nernst equation appeared to fit the redox titration data better when 1 electron equivalent was used ($n = 1$, dashed lines), although the same values for E_m were determined. The EPR method used in this work does not provide information regarding the number of electrons, although this observation may indicate that there has been a separation in the E_m values for the P^{2+}/P^{1+} and P^{1+}/P^N couples. It is evident that when the MoFe protein docks to the Fe protein, a large shift (−80 mV) is induced in the E_m of the P^{2+}/P^N cluster couples.

Finally, it was of interest to establish the effect of Fe protein−MoFe protein complex formation on the E_m for FeMoco (M-center). During catalysis, the M-cluster is proposed to be reduced beyond the resting state (M^N) by multiple electrons, with the more reduced states being referred to as E_1, E_2, etc. (*47*). As these reduced states are not accessible for redox titrations, we examined more oxidized states of the M-center instead. These more oxidized states of the M-center could be monitored by changes in EPR signal intensity in going from the reduced ($S = {}^3/_2$, M^N) state to an oxidized ($S = 0$, M^{ox}) state (*30*). Mediated redox titrations were performed on the $M^{ox/}M^N$ couple for both the MoFe protein alone and for the MoFe protein when complexed to the L127Δ Fe protein. No detectable differences in the E_m values (−52 mV) for these oxidation states of the M-clusters were observed when the complexed and noncomplexed states were compared. The measured E_m value is within the experimental error of ±10 mV of the published value of −42 mV (*30*). Thus, Fe protein−MoFe protein complex formation has negligible effects on the E_m of the M^{ox}/M^N couple.

DISCUSSION

The results of the present study demonstrate that formation of an Fe protein−MoFe protein complex results in significant changes in the midpoint potentials of two of the three nitrogenase metal centers, leading to an increase in the driving force for electron transfer reactions through nitrogenase. These results can be discussed in the context of three important questions about the nitrogenase mechanism: (i) how does Fe protein−MoFe protein complex formation influence the midpoint potentials of the two metal centers, (ii) how do these changes in midpoint potential affect electron transfer through nitrogenase to substrates, and (iii) what is the role of MgATP hydrolysis in altering the midpoint potentials of the clusters and in accelerating electron transfer?

Changes in the Properties of the Metal Centers of Nitrogenase. A clear picture is emerging of the nature of the Fe protein−MoFe protein docking interactions from recent X-ray crystallographic analyses of two different stable nitrogenase complexes (*11*, *48*). The 2-fold symmetry axis about the [4Fe-4S] cluster of the Fe protein becomes paired with the MoFe protein's pseudosymmetry axis through a P-cluster at an $\alpha\beta$-subunit interface. The binding of these two proteins in this orientation appears to result in a significant decrease in the solvent accessibility for both the Fe protein [4Fe-4S] cluster and the MoFe protein P-cluster (Figure 5). No changes in the environment of FeMoco are observed between the noncomplexed and Fe protein complexed MoFe protein. The decrease in solvent accessibility for two of the metal centers would be consistent with a lowering of the midpoint potentials for these metal centers. While there is still considerable debate about the factors that control the midpoint potentials of metal centers bound to proteins, three factors are generally accepted to participate: (i) solvent access to the metallocenter, (ii) amino acid side chain interactions with the metallocenter (e.g., hydrophobic side chains), and (iii) protein backbone amide dipole (including, but not limited to, hydrogen bonding) interactions with the metallocenter (*49*). From current models for the Fe protein−MoFe protein complex, it is not possible to define the factors which result in the lowering of the E_m of the [4Fe-4S] cluster upon complex formation. Certainly the overall decrease in solvent accessibility of the [4Fe-4S] cluster within the Fe protein−MoFe protein complex would be consistent with a negative shift in the midpoint potential. Studies with model [Fe-S] clusters have demonstrated that replacement of water as solvent with an organic solvent results in large negative shifts in midpoint potential (*50*, *51*).

The impact of Fe protein−MoFe protein docking appears to be similar for the P-clusters of the MoFe protein. Again, the factors which contribute to the lowering of the E_m are not known, but the decrease in the water solvent access to the P-clusters within the protein−protein complex is expected to result in a negative shift in the midpoint potential, consistent with the −80 mV shift observed. In contrast to the changes observed in the P-cluster and [4Fe-4S] cluster protein environments, no change in the FeMoco (M-center) protein environment is observed in either nitrogenase complex structure (*11*, *48*). The lack of change in the midpoint potential of the $M^{ox/N}$ couple in the protein−protein complex is consistent with the lack of changes in the structure. A more detailed analysis of the protein factors (e.g., solvent access and dipole interactions) that are regulating the midpoint potentials of the metal centers of nitrogenase upon component protein complex formation should be possible with the completion of a high-resolution structure for the L127Δ Fe protein−MoFe protein complex (Peters, Lan-

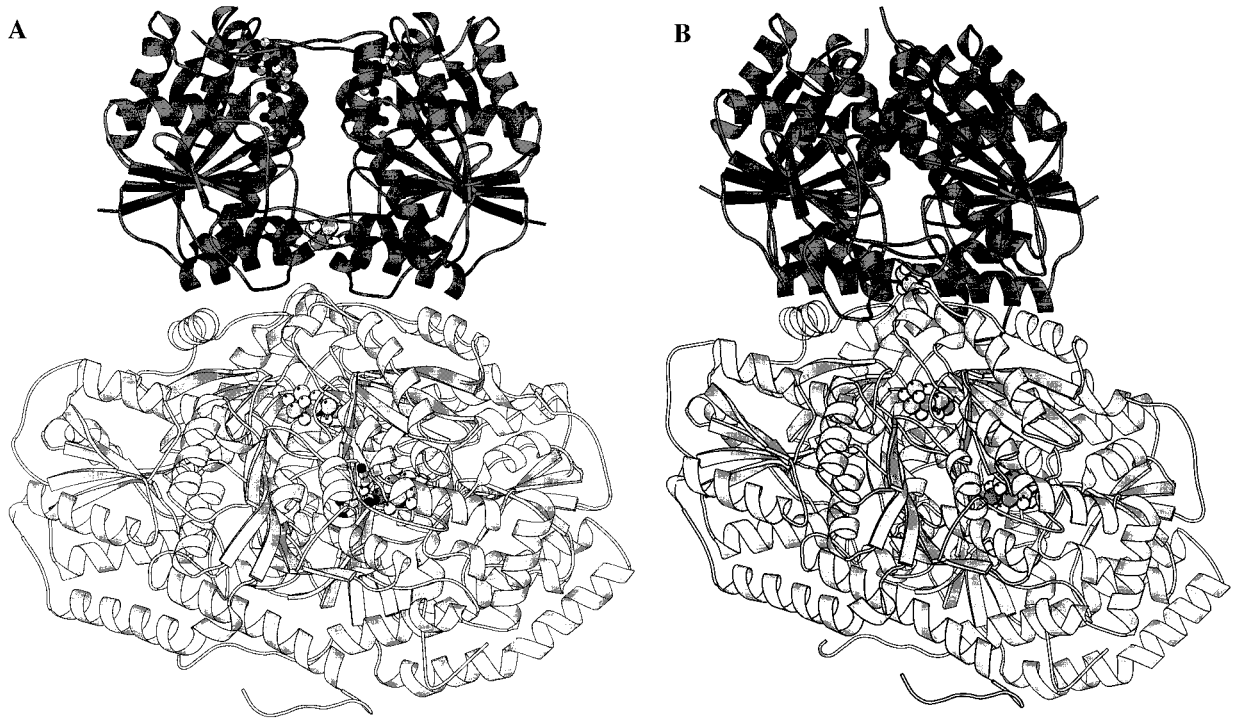

FIGURE 5: Structures of nitrogenase. The views show one half of the nitrogenase complex with the Fe protein on top and the MoFe protein on bottom either prior to protein−protein docking interactions (panel A) or within a nitrogenase Fe protein−MoFe protein complex (panel B). The [4Fe-4S] cluster, P-cluster, and M-center (from top to bottom) are presented as sphere models. The protein is presented as ribbons of the α carbon trace. The coordinates were taken from the X-ray crystal structures of the Fe protein and MoFe protein alone (*12*, *21*) or from an AlF_4^--MgADP stabilized Fe protein−MoFe protein complex (*11*). The figures were made with the program MOLSCRIPT (*62*).

Scheme 1

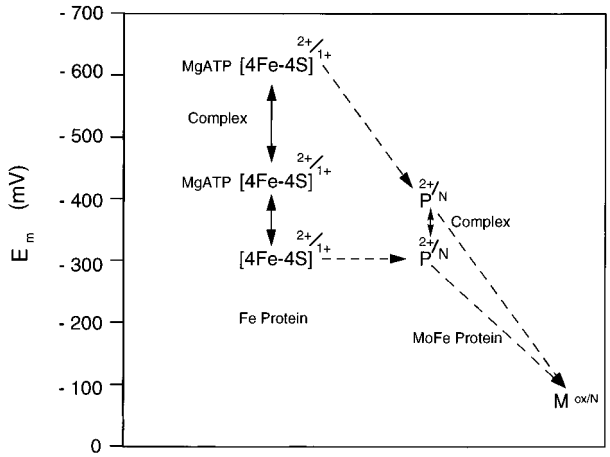

zilotta, Ryle, Howard, Seefeldt, and Rees, personal communication).

Implications for Intercomponent Electron Transfer in Nitrogenase. It is clear from the results of the present work that L127Δ Fe protein−MoFe protein docking results in a significant increase in the thermodynamic driving force for electron transfer from the [4Fe-4S] cluster to FeMoco. The relationships between the various redox states of the three nitrogenase metal centers is illustrated graphically in Scheme 1. The docking of L127Δ Fe protein to the MoFe protein results in a −200 mV change in the midpoint potential of the [4Fe-4S] cluster. This shift in potential is in addition to the −120 mV shift induced by deletion of Leu 127 of the Fe protein when compared to the wild-type Fe protein (*34*). The deletion of Leu 127 is thought to mimic the protein conformational changes normally induced by MgATP binding to the Fe protein, which also results in the same −120 mV change in the E_m for the [4Fe-4S] cluster (*34*). Thus, from the present results, it would appear that the combination of nucleotide binding to the Fe protein and Fe protein docking to the MoFe protein could result in a −320 mV shift in the E_m for the [4Fe-4S] cluster. Part of the energy of nucleotide binding and Fe protein docking to the MoFe protein must be coupled to this negative shift in the [4Fe-4S] cluster midpoint potential, resulting in the [4Fe-4S] cluster becoming a stronger reductant.

Similarly, Fe protein−MoFe protein docking significantly lowers the midpoint potential of the $P^{2+/N}$ cluster couple by −80 mV. As stated earlier, it is not clear which redox couples of the P-cluster are relevant to electron transfer reactions in nitrogenase, although there is growing evidence that the $P^{2+/N}$ couple is probably involved (*24*). The midpoint potential measured for the $P^{2+/N}$ couple within the nitrogenase complex of −390 mV would be consistent with the P-clusters as intermediate electron transfer units between the [4Fe-4S] cluster and the M-center. Again, the protein−protein docking energy appears to be coupled to a negative shift in the P-cluster midpoint potential, resulting in a larger driving force for electron transfer to the M-center.

The M-center couple used in the current work is unlikely to be catalytically relevant. It is expected that more reduced states of the M-cluster are involved in the nitrogenase mechanism, although there is no direct evidence for the existence of such reduced states. In addition, such reduced states of the M-center are not readily accessible for redox titrations. Thus, the $M^{ox/N}$ couple used in the present work was chosen as it provides an accessible couple that could be used as a starting place to understand the effects of Fe protein−MoFe protein docking on the properties of the M-center. The lack of any changes in the midpoint potential of the $M^{ox/N}$ couple would suggest a similar lack of effect

on other redox couples of the M-center. Thus, while the overall ΔE_m for the electron transfer reaction from the [4Fe-4S] cluster to the M-center of −600 mV observed in the present study is likely to change depending on the midpoint potential of the relevant M-center couple, it is clear that the Fe protein−MoFe protein docking event increases the driving force for electron transfer through nitrogenase by affecting the midpoint potentials of the [4Fe-4S] cluster and the P-clusters.

The observed effects of Fe protein−MoFe protein docking on the properties of the nitrogenase metal centers appear to contribute to an emerging theme for electron transfer protein partners. There are now a handful of examples that show that protein−protein complex formation influences the midpoint potentials of protein bound redox active centers to favor intercomponent electron transfer. For example, the midpoint potential of the [Fe-S] cluster of ferredoxin is observed to shift by −27 to −90 mV when this protein docks to a physiological electron transfer partner, ferredoxin-$NADP^+$ oxidoreductase (*52*−*54*). Similarly, protein−protein complex formation has been observed to result in favorable shifts in midpoint potentials of redox centers in the methylamine dehydrogenase and amicyanin (*55*), photosystem I and plastocyanin (*56*), and methane monooxygenase reductase and methane monooxygenase hydroxylase (*57*) complexes. Despite the availability of X-ray crystal structures for a cytochrome *c*−cytochrome *c* peroxidase complex (*58*), a methylamine dehydrogenase−amicyanin complex (*59*), and a methylamine dehydrogenase−amicyanin−cytochrome c complex (*60*), a detailed understanding of how protein−protein complex formation influences the midpoint potential of the redox centers has not emerged. The −200 mV shift in E_m observed in the present work for the L127Δ Fe protein [4Fe-4S] cluster is about twice as large as any other reported midpoint potential shift resulting from protein−protein complex formation. Such a large shift may be necessitated by the large activation energy for the N_2 reduction reaction (*61*).

Roles of MgATP Hydrolysis. An important observation from the current work is that, while primary electron transfer is observed to occur readily from the L127Δ Fe protein to the MoFe protein, the second electron transfer event is not observed. The primary electron transfer reaction is complete in 20 s, while no secondary electron transfer was observed even after 10 min (data not shown). In other words, after the L127Δ Fe protein has transferred the first electron to the MoFe protein, the second electron transfer event is either no longer thermodynamically or kinetically favorable. This observation may point to a role for MgATP hydrolysis in the second electron transfer reaction. It is possible that the energy of MgATP hydrolysis is necessary to promote the second electron transfer event or to influence downstream electron transfer reactions. This then leads to a developing consensus model for the function of MgATP hydrolysis that suggests that MgATP hydrolysis is related to nucleotide induced protein structural changes. The idea is that during the course of MgATP hydrolysis to MgADP + Pi, the protein conformation is constantly changing. This continuum of conformational changes can be thought of as having intermediate states of: Fe protein $(MgATP)_2$ → Fe protein $(MgADP + Pi)_2$ → Fe protein $(MgADP)_2$. What is clear is that the initial state with MgATP bound and the final state with MgADP bound have very different protein conformations (*7*). Thus, it seems reasonable to conclude that, as the nitrogenase Fe protein relaxes from the MgATP-bound state to the MgADP-bound state, the different protein conformations will influence the midpoint potentials of the nitrogenase metal centers. Given the intimate contact made between the Fe protein and the MoFe protein in the docked state, it is reasonable to assume that these nucleotide induced protein conformational changes will impact both the Fe protein [4Fe-4S] cluster and the MoFe protein P-clusters.

Thus, the nitrogenase mechanism appears to involve a series of protein conformations in both the Fe protein and the MoFe protein, with MgATP hydrolysis acting as a timing mechanism that couples the energtics of the hydrolysis events to changes in the protein conformations and consequently to changes in the properties of the metal centers. It is not clear what state in this continuum of conformations that the L127Δ Fe protein−MoFe protein represents, but the fact that this complex is competent for intercomponent electron transfer suggests that it does represent at least one of these states. It is now necessary to trap other conformational states of the nitrogenase complex in order to examine the properties of the metal centers to gain further insights into the role of MgATP in the electron transfer mechanism.

ACKNOWLEDGMENT

We thank Professor Vernon D. Parker for providing *N*,*N*′-propane-2,2′-dipyridinium, Jeannine M. Chan for providing purified *A. vinelandii* flavodoxin II, and Matthew J. Ryle for technical assistance. We also thank Professor Douglas C. Rees, Dr. John W. Peters, and Dr. Mike Stowell for helpful discussions about the nitrogenase complex structures.

REFERENCES

1. Howard, J. B., and Rees, D. C. (1994) *Annu. Rev. Biochem. 63*, 235−264.
2. Mortenson, L. E., Seefeldt, L. C., Morgan, T. V., and Bolin, J. T. (1993) *Adv. Enzymol. 67*, 299−374.
3. Peters, J. W., Fisher, K., and Dean, D. R. (1995) *Annu. Rev. Microbiol. 49*, 335−366.
4. Seefeldt, L. C., and Dean, D. R. (1997) *Acc. Chem. Res. 30*, 260−266.
5. Hageman, R. V., and Burris, R. H. (1978) *Proc. Natl. Acad. Sci. U.S.A. 75*, 2699−2702.
6. Thorneley, R. N. F., and Lowe, D. J. (1983) *Biochem. J. 215*, 393−403.
7. Burgess, B. K., and Lowe, D. J. (1996) *Chem. Rev. 96*, 2983−3011.
8. Duyvis, M. G., Wassink, H., and Haaker, H. (1996) *J. Biol. Chem. 271*, 29632−29636.
9. Shah, V. K., and Brill, W. J. (1977) *Proc. Natl. Acad. Sci. U. S. A. 74*, 3249−3253.
10. Hawkes, T. R., McLean, P. A., and Smith, B. E. (1984) *Biochem. J. 217*, 317−321.
11. Schindelin, H., Kisker, C., Schlessman, J. L., Howard, J. B., and Rees, D. C. (1997) *Nature 387*, 370−376.
12. Georgiadis, M. M., Komiya, H., Chakrabarti, P., Woo, D., Kornuc, J. J., and Rees, D. C. (1992) *Science 257*, 1653−1659.
13. Watt, G. D., Wang, Z. C., and Knotts, R. R. (1986) *Biochemistry 25*, 8156−8162.
14. Watt, G. D., and Reddy, K. R. N. (1994) *J. Inorg. Biochem. 53*, 281−294.
15. Zumft, W. G., Palmer, G., and Mortenson, L. E. (1973) *Biochim. Biophys. Acta 292*, 413−421.
16. Walker, G. A., and Mortenson, L. E. (1974) *Biochemistry 13*, 2382−2388.
17. Meyer, J., Gaillard, J., and Moulis, J. M. (1988) *Biochemistry 27*, 6150−6156.

18. Lanzilotta, W. N., Holz, R. C., and Seefeldt, L. C. (1995) *Biochemistry 34*, 15646−15653.
19. Stephens, P. J., McKenna, C. E., Smith, B. E., Nguyen, H. T., McKenna, M. C., Thomson, A. J., Devlin, F., and Jones, J. B. (1979) *Proc. Natl. Acad. Sci. U.S.A. 76*, 2585−2589.
20. Ryle, M. J., Lanzilotta, W. N., Mortenson, L. E., Watt, G. D., and Seefeldt, L. C. (1995) *J. Biol. Chem. 270*, 13112−13117.
21. Kim, J., and Rees, D. C. (1992) *Nature 360*, 553−560.
22. Ma, L., Brosius, M. A., and Burgess, B. K. (1996) *J. Biol. Chem. 271*, 10528−10532.
23. Peters, J. W., Fisher, K., Newton, W. E., and Dean, D. R. (1995) *J. Biol. Chem. 270*, 27007−27013.
24. Lowe, D. J., Fisher, K., and Thorneley, R. N. F. (1993) *Biochem. J. 292*, 93−98.
25. Lanzilotta, W. N., and Seefeldt, L. C. (1996) *Biochemistry 35*, 16770−16776.
26. Smith, B. E., and Lang, G. (1974) *Biochem. J. 137*, 169−180.
27. Huynh, B. H., Munck, E., and Orme-Johnson, W. H. (1979) *Biochim. Biophys. Acta 576*, 192−203.
28. Münck, E., Rhodes, H., Orme-Johnson, W. H., Davis, L. C., Brill, W. J., and Shah, V. K. (1975) *Biochim. Biophys. Acta 400*, 32−53.
29. Peters, J. W., Stowell, M. H. B., Soltis, S. M., Finnegan, M. G., Johnson, M. K., and Rees, D. C. (1997) *Biochemistry 36*, 1181−1187.
30. Pierik, A. J., Wassink, H., Haaker, H., and Hagen, W. R. (1993) *Eur. J. Biochem. 212*, 51−61.
31. Tittsworth, R. C., and Hales, B. J. (1993) *J. Am. Chem. Soc. 115*, 9763−9767.
32. Morgan, T. V., Mortensen, L. E., McDonald, J. W., and Watt, G. D. (1988) *J. Inorg. Biochem. 33*, 111−20.
33. Seefeldt, L. C., and Mortenson, L. E. (1993) *Protein Sci. 2*, 93−102.
34. Ryle, M. J., and Seefeldt, L. C. (1996) *Biochemistry 35*, 4766−4775.
35. Klugkist, J., Voorberg, J., Haaker, H., and Veeger, C. (1986) *Eur. J. Biochem. 155*, 33−40.
36. Hathaway, G. M., Lundak, T. S., Tahara, S. M., and Traugh, J. A. (1979) *Methods Enzymol. 60*, 495−511.
37. Chromy, V., Fischer, J., and Kulhanek, V. (1974) *Clin. Chem. 20*, 1362−1363.
38. Seefeldt, L. C., and Ensign, S. A. (1994) *Anal. Biochem. 221*, 379−386.
39. Lanzilotta, W. N., Fisher, K., and Seefeldt, L. C. (1996) *Biochemistry 35*, 7188−7196.
40. Ryle, M. J., Lanzilotta, W. N., and Seefeldt, L. C. (1996) *Biochemistry 35*, 9424−9434.
41. Ashby, G. A., and Thorneley, R. N. F. (1987) *Biochem. J. 246*, 455−465.
42. Thorneley, R. N. F., and Deistung, J. (1988) *Biochem. J. 253*, 587−595.
43. Watt, G. D. (1979) *Anal. Biochem. 99*, 399−407.
44. Zimmermann, R., Münck, E., Brill, W. J., Shah, V. K., Henzl, M. T., Rawlings, J., and Orme-Johnson, W. H. (1978) *Biochim. Biophys. Acta 537*, 185−207.
45. Watt, G. D., Burns, A., Lough, S., and Tennent, D. L. (1980) *Biochemistry 19*, 4926−4932.
46. Johnson, M. K., Thomson, A. J., Robinson, A. E., and Smith, B. E. (1981) *Biochim. Biophys. Acta 671*, 61−70.
47. Thorneley, R. N. F., and Lowe, D. J. (1984) *Biochem. J. 224*, 903−909.
48. Peters, J. W., Lanzilotta, W. N., Ryle, M. J., Howard, J. B., Seefeldt, L. C., and Rees, D. C. (1997) (manuscript in preparation).
49. Jensen, G. M., Warshel, A., and Stephens, P. J. (1994) *Biochemistry 33*, 10911−10924.
50. Mayerle, J. J., Frankel, R. B., Holm, R. H., Ibers, J. A., Phillips, W. D., and Weiher, J. F. (1973) *Proc. Natl. Acad. Sci. U.S.A. 70*, 2429−2433.
51. Kassner, R. J., and Yang, W. (1977) *J. Am. Chem. Soc. 99*, 4351−4355.
52. Pueyo, J. J., Revilla, C., Mayhew, S. G., and Gomez-Moreno, C. (1992) *Arch. Biochem. Biophys. 294*, 367−372.
53. Smith, J. M., Smith, W. H., and Knaff, D. B. (1981) *Biochim. Biophys. Acta 635*, 405−411.
54. Batie, C. J., and Kamin, H. (1981) *J. Biol. Chem. 256*, 7756−7763.
55. Gray, K. A., Davidson, V. L., and Knaff, D. B. (1988) *J. Biol. Chem. 263*, 13987−13990.
56. Drepper, F., Hippler, M., NItschke, W., and Haehnel, W. (1996) *Biochemistry 35*, 1282−1295.
57. Liu, Y., Nesheim, J. C., Paulsen, K. E., Stankovich, M. T., and Lipscomb, J. D. (1997) *Biochemistry 36*, 5223−5233.
58. Pelletier, H., and Kraut, J. (1992) *Science 258*, 1748−1755.
59. Chen, L., Durley, R., Poliks, B., Hamada, K., Chen, Z., Mathews, F. S., Davidson, V. L., Satow, Y., Huizinga, E., Vellieux, F. M. D., and Hol, W. G. J. (1992) *Biochemistry 31*, 4959−4964.
60. Chen, L., Durley, R. C. E., Mathews, F. S., and Davidson, V. L. (1994) *Science 264*, 86−90.
61. Alberty, R. A. (1994) *J. Biol. Chem. 269*(10), 7099−7102.
62. Kraulis, P. J. (1991) *J. Appl. Crystallogr. 24*, 946−950.

BI9715371